POST-DIGITAL - European Training Network on Post-Digital Computing [GA860360]

Document Details

Title	Deliverable 4.1 Simulation and experimental study of application of photonic reservoir computing to non-linear optical channel equalization
Deliverable number	D4.1
Deliverable Type	Report (public)
Deliverable title	Simulation and experimental study of application of photonic reservoir computing to non-linear optical channel equalization
Work Package	WP4- Benchmarking and applications
Description	Simulation and experimental study of application of photonic reservoir computing to non-linear optical channel equalization
Deliverable due date	30/09/2022
Actual date of submission	11/11/2022
Lead beneficiary	Aston
Version number	V1.0
Status	Final

Dissemination level

PU	Public	X
CO	Confidential, only for members of the consortium (including Commission Services	

Project Details

Grant Agreement	860360
Project Acronym	POST-DIGITAL
Project Title	POST-DIGITAL - European Training Network on Post-Digital Computing
Call Identifier	H2020-MSCA-ITN-2019
Project Website	https://postdigital.astonphotonics.uk/
Start of the Project	1 April 2020
Project Duration	48 months

This project has received funding from the European Union's Horizon 2020 research and innovation programme under the Marie Skłodowska-Curie grant agreement No 860360

Table of Contents

1 Introduction

Biological brains perform extremely complicated tasks and carry out these computations with a remarkably low energy budget. For example, the human brain categorizes, predicts and creates with a power consumption only about 20 W. This fact has turned them into a benchmark in the data processing context and has inspired the creation of new technologies, as it is the case of Artificial Intelligence (AI) [1, 2].

AI has the potential to drastically change almost every aspect of our lives thanks to its application to a wide variety of fields, as for example medicine or transportation. The past six years has seen a renaissance in AI consequence of the development of Deep learning with artificial neural networks (NN), which is a particular type of algorithm inspired in the brain. Thanks to this, incredible performances have been achieved in tasks as for example image recognition or language translation, among others [3–5].

Although current digital computers are capable of high-precision calculations, they expend vast amounts of energy when carrying out cognitive tasks similar to those the brain is so successful at [1, 3, 5]. This is a consequence of the differences at the physical and architectural level between these two systems. Some particular examples of these differences are the use of synapses and neurons, instead of memory blocks and transistors; taking advantage of the stochasticity of cells, instead of relying on high precision circuits; the use of both binary and analog coding, instead of just binary coding; relying on asynchronous communication, instead of the single clock for synchronous communication; the serialised von Neumann architecture in contrast to the brain's parallel one [1, 3].

Moreover, in addition to the drawbacks related to the energy consumption, conventional computing systems can no longer satisfy the growing computing demands, as Moore's law (exponential hardware scaling) is slowing down [3, 6].

All this has inspired the development of a new discipline known as Neuromorphic Computing, which main objective is building large scale "bio-inspired" hardware that reproduces ANN's topology in order to achieve computational efficiencies similar to those of a human brain, as well as maximal computing performance [3, 7]. Thus, it would make possible to overcome the performance limitations inherent in traditional von Neumann architectures [3]. On the other hand, a transformation is taking place within this field, where a branch known as neuromorphic photonics is becoming more relevant. The main reason is that by using photonics, it is possible to achieve high energy efficiency, large bandwidth and low latencies, overcoming fundamental issues in digital and analog electronics [2, 3, 5].

Within the context of Neuromorphic Computing, one of its major exponents is the framework known as Reservoir Computing (RC) [8]. Its main feature is the use of a Recurrent Neural Network (RNN) known as reservoir that maps the inputs into a high-dimensional space and a readout for processing the high-dimensional states in the reservoir. As the training process only takes place in the readout, the reservoir is a very good option for hardware implementation. Thus, several physical systems, substrates, and devices have been proposed for this purpose. Moreover, such physical reservoir computing has attracted increasing attention in diverse fields of research [8, 9]. One of them is the mitigation of non-linear impairments in optical communication systems.

2 The Nonlinearity Problem in Optical Fiber Communications

2.1 Propagation of Light in the Fiber

The fundamental equation used to describe the propagation of light along an optical fiber is commonly referred to as the nonlinear Schrödinger equation (NLSE) [10] and can be derived directly from the Maxwell equations, which describe the foundations of electricity and magnetism [11]. The NLSE reads as:

$$\frac{\partial E}{\partial z} = (\hat{L} + \hat{N})E, \tag{1}$$

where E is the electrical field as a function of the propagation distance z and time t. $\hat{D}$ and $\hat{N}$, describe the linear and nonlinear parts of the NLSE, which are given by:

$$\begin{aligned} \hat{L} &= \underbrace{-\frac{\alpha}{2}}_{\text{loss}} - \underbrace{\frac{j\beta_2}{2}\frac{\partial^2}{\partial t^2}}_{\text{GVD}} + \underbrace{\frac{j\beta_3}{6}\frac{\partial^3}{\partial t^3}}_{\text{GVD slope}}, \\ \hat{N} &= \underbrace{j\gamma|E|^2}_{\text{Kerr effect}}, \end{aligned} \tag{2}$$

where α, $\beta_{2,3}$, and γ are the attenuation, the group velocity dispersion (GVD), and the nonlinear coefficient, respectively. If we substitute $\hat{L}$ and $\hat{N}$ from Eq. (2) into Eq. (1), it provides the explicit form of the NLSE:

$$\frac{\partial E}{\partial z} + \frac{\alpha}{2}E + \frac{j\beta_2}{2}\frac{\partial^2 E}{\partial t^2} - \frac{j\beta_3}{6}\frac{\partial^3 E}{\partial t^3} = j\gamma|E|^2E. \tag{3}$$

Eq. (3) is suitable to model optical fiber transmission when transmission along a single-polarization only is explored, e.g., intensity-modulation with direct-detection systems [10]. However, a coherent transceiver employs advanced digital signal processing (DSP) which enables detecting a dual-polarization signal, thus doubling the spectral efficiency of the system. In this context, the linear and non-linear interactions between the two signal polarizations must be taken into account. Consequently, the NLSE of Eq. (3) is extended in a vectorized form:

$$\begin{aligned} \frac{\partial E_X}{\partial z} &= \underbrace{-\frac{\alpha}{2}E_X + \frac{j\beta_2}{2}\frac{\partial^2}{\partial t^2}E_X - \frac{j\beta_3}{6}\frac{\partial^3}{\partial t^3}E_X}_{\text{linear part}} \\ &\quad \underbrace{-j\gamma\frac{8}{9}\left(|E_X|^2 + |E_Y|^2\right)E_X}_{\text{nonlinear part}}, \\ \frac{\partial E_Y}{\partial z} &= -\frac{\alpha}{2}E_Y + \frac{j\beta_2}{2}\frac{\partial^2}{\partial t^2}E_Y - \frac{j\beta_3}{6}\frac{\partial^3}{\partial t^3}E_Y \\ &\quad -j\gamma\frac{8}{9}\left(|E_X|^2 + |E_Y|^2\right)E_Y. \end{aligned} \tag{4}$$

This pair of equations is commonly referred to as “the Manakov equation”, and it involves both polarization states. Here, E_X and E_Y represent the two orthogonal polarization components of the electric field E. In addition to the two polarizations, Eq. 4 properly averages the impact of residual birefringence that leads to fast polarization changes. Since the polarization state of the electric field changes rapidly, the resulting nonlinearities do not correspond to the ones from a linearly or circularly polarized field but to an average over the entire Poincaré sphere.

The previous equations do not take into account, for example, stimulated Raman scattering (SRS). The SRS is a nonlinear effect that leads to the depletion of power from short to long wavelengths, achieving its maximum efficiency when the signals are separated by $\sim$100 nm. The Raman effect has mainly been explored to design distributed Raman amplifiers. Indeed, the SRS impact is usually negligible in C-band only systems, which occupy $\sim$35 nm. However, with the advent of ultra-wideband optical systems, SRS will become the main transmission impairment in optical networks [12].

2.2 Channel Capacity Limitations caused by Nonlinear Kerr Effect

The non-linear part of Eq. (4) imposes a severe limitation on the maximum achievable throughput in an optical fiber. In fact, the information theory indicates that the capacity of a linear channel increases monotonically by raising the transmitted signal power (or rather signal-to-noise ratio, SNR) [13]. This theoretical limit is also commonly referred to as Shannon's limit. However, in fiber optics, this tendency does not hold because the term $\left(|E_X|^2 + |E_Y|^2\right) E_{X,Y}$ becomes progressively more important as the transmitted signal power increases, thus causing phase distortions that limit the maximum throughput in the network [14]. Consequently, there is an optimal optical signal power that balances the achievable maximum SNR and the signal distortion induced by the optical fiber's nonlinear behavior.

These peculiar aspects of fiber propagation have been widely investigated, together with mitigation techniques, in both the optical and digital domains. The next subsection provides a brief overview of some studies carried out to mitigate the nonlinear Kerr effect in the digital domain. Nevertheless, a more complete review can be found in, e.g., Ref. [15].

2.3 Mitigation of Fiber Propagation Effects

Eq. (4) is a multi-domain differential equation that does not have a closed-form solution. A possible way to solve it is to apply the "Split-step Fourier method" (SSFM). This method assumes that the linear ($\hat{L}$) and Kerr nonlinear ($\hat{N}$) effects can be separated and solved independently when a propagation step-size small enough is considered, alternating between them along the optical fiber. A more detailed description of this approach can be found in Refs. [16, 17]. The absence of an analytical solution for the Manakov equations makes the perfect compensation of transmission effects very difficult. Additionally, and as an example, the loss of the phase information severally limits the compensation of transmission effects in direct-detection-based receivers (RXs). However, thanks to coherent detection, the amplitude and phase of the transmitted signal can be simultaneously detected at the RX input, which enables applying enhanced DSP algorithms to at least partially compensate for transmission effects. Indeed, the linear effects, such as GVD and polarization mode dispersion (PMD), can be fully compensated for in the electronic domain by using a frequency domain equalizer in conjunction with a multiple-input multiple-output (MIMO) equalizer. On the other hand, the compensation of the Kerr nonlinear effects that induce a self- and cross-phase modulation (SPM and XPM, respectively) on the transmitted signal is much more difficult.

The full compensation of the Kerr effect is troublesome as the equalizer would require complete knowledge of the propagation channel itself (for the SPM compensation), of the neighboring channels (for the XPM compensation), and of the amplified spontaneous emission (ASE) noise (intertwining with both SPM and XPM). Nevertheless, several methods have been proposed to digitally mitigate nonlinearities. Among them, the most relevant ones that are worth to be ex-

plicitly mentioned and described are: 1) maximum likelihood sequence estimation (MLSE); 2) Volterra-series based equalizers; 3) DBP; 4) NN-based techniques (we provide some respective references below).

MLSE is the optimal method as long as there is no limitation on the number of states of the trellis code, as shown by [18] for coherent- and by [19] for direct-detection systems. However, complying with this limitation means that it may become too complex and its potential commercial application ended with 10 Gb/s systems [20], where it has been mainly used to compensate for GVD. At current high symbol rates, it seems unrealistic to implement a sufficiently low-power-consumption MLSE equalizer.

Volterra equalizers were proposed in the '70s for satellite communications [21], and provide a nonlinear version of the widely used finite impulse response (FIR) filters. They are based on the mathematical technique developed by Vito Volterra, which is an extension of Taylor's series but for a general function. Volterra equalizers can result in significant improvements in transmission quality [22, 23] but, like in the case of MLSE, their complexity is too high for realistic implementation.

DBP[1] gained momentum about a decade ago when the article by Ip and Kahn [24] was published. The main idea behind DBP is to extend the MIMO equalizer by adding a nonlinear part, so that DBP would invert the nonlinear and linear parts of Eq. 4 by applying the SSFM and solving the propagation equation (4) backward at the RX. However, DBP is effective only when combined with coherent detection and is deemed as being relatively complex for realistic implementation. Several methods have been proposed to simplify the DBP concept [25–27], but its complexity is still considered to be high.

NNs are intrinsically nonlinear and, therefore, match well with the type of effects we want to mitigate. Moreover, NNs can still be employed even in the absence of link information or in cases where the system configuration has changed as they obtain the required information directly from the received signal. However, NNs can be quite complex, often even more complex than DBP [28], which is the main limitation when employing them in practice. Thus, physical implementation of RC presents itself as a promising solution to this problem.

3 Optical Implementation of Reservoir Computing

On the way of looking for a NN suitable for hardware implementation, the attraction has focused on the foundation of echo state networks (ESN) [29] and liquid state machines (LSM) [30]. They proved that a NN can work well without optimizing most of its weights, and they formed the already mentioned computational framework called "Reservoir Computing", where the input signals are mapped to a higher dimensional space using the dynamics of a set (so-called "reservoir") of multiple nonlinear nodes.

We will discuss the principle and operation of the RC with the ESN as a representative of the framework. The architecture of an ESN which consists of an input layer, a reservoir layer and an output layer, can be shown in Fig. 1. In ESN, a real M-dimension training input data can be expressed as a vector $\boldsymbol{u}(n) \in \mathbb{R}^M$ at the discrete-time instant n, and a real K-dimension desired output can be given by a vector $\boldsymbol{y}(n) \in \mathbb{R}^K$. The ESN's reservoir with N nodes has its dynamics described through the vector $\boldsymbol{x}(n) \in \mathbb{R}^N$ which is updated at each time step as following:

[1] Not to be confused with the backpropagation through the NN layers used for the training of NNs.

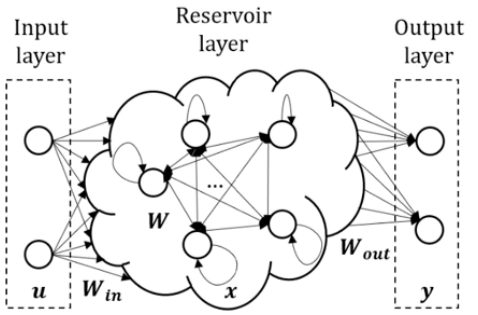

Figure 1: ESN architecture

$$\boldsymbol{x}(n+1) = (1-\alpha)\boldsymbol{x}(n) + \alpha f(\boldsymbol{W}_{in}\boldsymbol{u}(n+1) + \boldsymbol{W}\boldsymbol{x}(n)) \tag{5}$$

where $\alpha \in (0;1]$ is the leaking rate which represents the exponential decay of the reservoir and emulates the physical implementation. The input is fed to the reservoir through a linear transformation whose coefficients are given by the input weight matrix $\boldsymbol{W}_{in}$. The interconnection matrix $\boldsymbol{W}$ is the reservoir's adjacency matrix and $f(.)$ is the activation function of the nodes within the reservoir. Both $\boldsymbol{W}_{in}$ and $\boldsymbol{W}$ are randomly initialized and kept fixed during entirely the training and test phases. The output layer of the ESN usually uses a linear activation transformation onto the reservoir states:

$$\boldsymbol{y}(n) = \boldsymbol{W}_{out}\boldsymbol{x}(n) \tag{6}$$

In a typical ESN training process, all the weights except the output weights $\boldsymbol{W}_{out}$ are initialized before the reservoir states are updated using Eq (5). The learning only performs on the output layer for the linear relationship in Eq (6) that can be considered a simple linear regression problem. We thus do not need to perform the computationally expensive backpropagation algorithm as we do in RNN. The ESN has been proven to give decent performance on supervised time-dependent data tasks, such as nonlinear equalization [31], speech recognition, handwriting recognition and financial forecasting [32]. The random initialization in the ESN allows the reservoir to be realized by physical dynamic systems, so its simplified design and reduced expensive training requirement help enabling its potential in realistic implementation.

Many efforts have been made on optical realization of RC although the first designs were introduced last decade. We can classify these previous works in two types based on how they organize the internal nodes within the reservoir. The first one is called spatially distributed reservoir systems where their topologies follow the conventional neural connections of multiple photonic elements which play roles as neural nodes. The other type is regarded to time-delay reservoir systems where the internal nodes are virtually created by utilizing a single nonlinear node coupled with a feedback loop.

3.1 Reservoir with multiple photonic elements

The first system is built based on a network of SOAs on chip [33], [34] where the nonlinear characteristics of a SOA is exploited to resemble the hyperbolic tangent (tanh) activation function. The system where SOAs are connected in a waterfall topology is tested through a numerical modelling, and its performance even shows a better result in some tasks than the traditional

tanh-based reservoir. Having had encouraging results on numerical simulation, further efforts are made to create a first photonic RC [35]. However, these SOA-based approaches have a same issue in power efficiency due to exploiting the nonlinear regime of SOA characteristics and limited processing time due to carrier life time. To overcome these limitations of a SOA, a design of reservoir with only passive photonic components, namely waveguides, splitters, and combiners, is developed [36]. This reservoir is energy efficient but totally linear, and the nonlinearity is only introduced at the readout layer where a photodiode converts complex amplitudes into electrical power levels through a quadratic relationship. It is thus still an optoelectronic system, and the goal about an all-optical RC could not be achieved. The advantage of this system is broadband due to the presence of passive elements, while its bulky size as scaling out to more nodes and the capability to extracting the reservoir nodes' output in parallel.

3.2 Reservoir with a single photonic element

The original idea of time delay reservoir started from a concept of a simplified reservoir topology where internal nodes of an ESN are connected in a circle [37]. It showed that an ESN with a simple circular topology can have a similar performance compared to other conventional ESNs. Leveraging that, a concept of using a single nonlinear node with a feedback loop resembling of an ESN with circular topology is introduced [38], potentially paves the way for the development of the time-delay reservoir system. Time delay systems have some advantages over the spatially distributed systems that are capability to introduce a high dimension with many nodes while easing the complexity in hardware implementation.

3.2.1 Mach-Zehnder-based reservoir

In this setup, a Mach-Zehnder modulator (MZM) does not only play a role of modulating the incoming optical signal but also works as a nonlinear device (MZM has a squared-sin transfer function) for this time-delay setup [39] [40]. The MZM output then goes through a single mode fibre (SMF) before being detected by a photodetector (PD). A portion of the PD output is extracted to detect internal states within the reservoir, while the other is merged with the input data to become the modulating signal for the MZM and close the feedback loop. The system is then tested for various tasks of speech recognition, time series prediction, nonlinear equalization.

An autonomous version of this RC can be done by using a field-programmable gate array (FPGA) where the output weights are trained online [41] . Because FPGA is a digital electronic hardware, there should be some digital-to-analog and analog-to-digital conversions in the process.

3.2.2 Semiconductor optical amplifier-based reservoir

Building an all-optical RC has some advantages: avoiding back and forth conversions between electronic and optical domains because these are limited by noise and operating bandwidth. An all-optical RC can directly interface with the output of optical communication for nonlinear equalization. The first scheme is a time-delay system based on SOA whose saturation gain effect can be exploited for the reservoir nonlinearity [42] . The SOA is a preferred choice due to its compactness and ability to compensate for losses within the delay loop. The isolator is used to avoid any unnecessary backward reflection from the SOA, and the optical filter cancels

out any out-of-band noise from the SOA output. Two optical attenuators control the strengths of input and feedback signals fed to the reservoir in the next circles. The reservoir interconnections in this case can be mimicked by a desynchronization between the masking process and the feedback loop length.

3.2.3 Injection locked laser-based reservoir

The reservoir, in this scheme, consists of a semiconductor laser, an optical circulator which directs the light from the loop to the injected laser and back again to the loop and a polarization controller [43]. The nonlinearity is introduced by the semiconductor laser with feedback, and its high accuracy performance is tested on spoken digit recognition and chaotic time series prediction tasks and the processing speed can be at GBytes/s.

3.2.4 Fibre-based reservoir

A proposed fibre-optic RC, so-called fibre echo state network analogue (FESNA), which exploits the nonlinearity from a nonlinear optical loop mirror (NOLM), can unlock the operational bandwidth over 100 GHz and enable dual-quadrature processing feature [44]. In a step of increasing the process speed, a modified version, dispersion-managed FESNA (DM-FESNA), uses dispersion effect for weight mixing instead of using electrical elements [45].

The previous works focus on the physical implementation of the reservoir, so the input and output layers are supposed to be done offline. Therefore, the input and output weights should also be implemented in physical hardware to fully implement a RC [46]. This kind of computer can increase the energy efficiency as well as accelerates the processing speed. At the input layer, the input weights (or masks) are temporal multiplexed to multiply with the input signal. The input masks are thus fed to the RF port of the second MZM whose input port is injected with the input data. An optical attenuator monitors the masked input's strength as a realization of the input scaling parameter. However, due to the technical limitation of arbitrary waveform generator (AWG), this approach cannot introduce high dimension to the random masks and further efforts may be needed to resolve this issue. At the output layer, 30 percent of the reservoir output will detected by a PD for offline training which results in an optimal output weight matrix. The other 70 will go to a dual-output MZM driven by the newly learned output weight matrix. Its two outputs are then detected by two balanced photodiodes before filtered by a low-pass RLC filter.

4 Photonic reservoir computing for optical communications

Many RC-based designs listed in Section 2 have been used for the optical channel equalization tasks, and we will discuss about some notable works in this section.

An injection locked laser-based reservoir with 66 virtual nodes with feedback loop length of 66 ns was used for transmission data recovery of pulse-amplitude modulation (PAM) signals [47] where two transmission scenarios were tested: short reach network with 50 km of SMF at the speed of 25 Gb/s, and long haul network with 4000 km at 10 Gb/s. The reservoir-based equalizer was optimized by considering various window lengths of neighboring symbols, and it achieved the bit error rate (BER) performance more than one order of magnitude compared

to the linear classifier in both scenarios. The first scenario was also tested for the MZM-based reservoir scheme which returned even a slightly better BER [48]. It means the MZM-based scheme has a better computational capacity, but the injection locked laser-based scheme has a better reservoir bandwidth exploitation thanks to inertia node coupling. The same injection locked laser-based equalizer with 32 virtual nodes for transmission of PAM signals with 4 levels (PAM-4) were tested for two scenarios: 27 km at 56 Gb/s and 5.5km at 112 Gb/s [49]. The numerical results showed that the systems can maintain the BER under the hard-decision forward error correction (HD-FEC) threshold, while the linear classifier failed to do so. Experimental results verified the BER performance, but with slightly shorter distances of 21 km and 4.6 km respectively. A scheme with bandwidth enhancement was developed to enable the node spacing as small as 12 ps, consequently allowed us to use 80 virtual nodes with feedback loop delay of 0.96 ns [50]. Its performance on the signal recovery task for quadrature phase shift keying (QPSK) transmission of 180 km at 56 Gb/s returned a BER of around 10^{-3}.

A fiber-based reservoir, so-called fiber echo state network analogue (FESNA), was tested for the dual-quadrature signal recovery task [44]. The system in the test scenario was multi-level quadrature amplitude modulation (m-QAM) signal transmission of 100 km of SMF at 30 GBaud/s. The results showed one order of magnitude advantage over the linear equalizer in terms of BER for 64-QAM and 256-QAM cases. An all-optical version of FESNA, which can avoid electrical components for better operation bandwidth, was developed by adopting the dispersion compensating fiber (DCF) [45]. The new scheme, which is named dispersion-managed FESNA (DM-FESNA), showed 2 dB and 3 dB gain for 64-QAM and 256-QAM respectively at the BER level of 10^{-3}. The test scenario was then expanded to multi-channel transmission, namely 5 wavelength-division multiplexing (WDM) channels of 64-QAM, resulted in 1.2 dB peak gain over the linear equalizer [51].

An integrated photonic reservoir with swirl architecture connecting real nodes as 3x3 MMIs was also tested for the nonlinear equalization task [52]. In detail, the reservoir has 32 nodes connected in 4x8 configuration. Its result on the nonlinear mitigation task of 25 km PAM transmission at 32 Gb/s outperformed the linear equalizer, maintained a BER level below forward error correction (FEC) limit even with a high launched power up to 18 dBm.

In POST-DIGITAL project, ESR9 is working on the nonlinear equalization of 64-QAM signals transmitted as single-sideband (SSB) signals [53]. The signals are direct detected and the phase information is reconstructed using a Kramers Kronig (KK) receiver. For such a setup to work, the power of the SSB subcarrier must be significantly higher than the power of the signal. With such power, the fiber nonlinearities are strong and induce significant errors. In addition, the transmitter's modulator is also a nonlinear component which adds nonlinear distortion to the signal. To perform nonlinear equalization optically using RC, a 16-node integrated photonic reservoir is used. The reservoir is composed of 3-by-3 MMI's and interconnecting waveguides, making it a passive reservoir. The reservoir behavior is studied by adapting the length of the waveguides and the signal injection locations, which allows informing the design decisions for an optimum reservoir. They conclude that, for optimum behavior, the waveguide lengths should induce a time delay equal to half the symbol period. The optimum signal injection locations varied by the problem. The reservoir readout uses all 16 nodes to connect to complex weights, which is then passed to the receiver. The KK receiver behaves as a nonlinear element which elevates the reservoir performance due to this added nonlinearity in the readout. The system is simulated for inter/intra data center deployments, where lengths of up to 100 km are typical. VPI Photonics software is used to accurately model the transmitter and channel impairments. Chromatic dispersion is compensated for optically prior to the reservoir to ensure that the reservoir is targeted towards the compensation of nonlinear errors. The reservoir is

simulated using Photontorch. A system schematic is shown below in Figure 2. ESR 9 will carry out a secondment at Aston in 2023, during which the system will be used for non-linear impairments mitigation in optical communication systems.

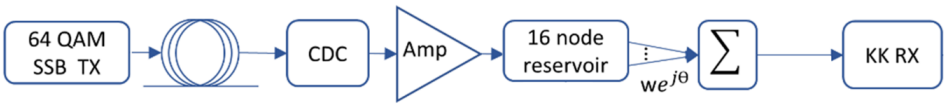

Figure 2: Schematic of simulated system deploying reservoir for nonlinear equalization and a Kramers-Kronig receiver for direct detection.
QAM: Quadrature-Amplitude Modulated; SSB Tx: Single Sideband Transmitter; CDC: Chromatic Dispersion Compensation; Amp: Amplifier; KK Rx: Kramers-Kronig Receiver

The optimization of the readout weights happens in two parts. For the first part, the weights are initialized by finding the linear solution which best approximates the target signal. Since this is a linear solution, the target signal before the receiver is used (i.e. before the nonlinear element is included in the solution). We term this Linear RC (L. RC). In the second part, the weights are then optimized by backpropagating through the receiver which improves the performance of the reservoir since the equalizer includes a nonlinear part now. We term this Nonlinear RC (NL RC).

Simulation results seen in Figure 3 show how L. RC and NL. RC perform in terms of testing BER over fiber lengths from 20 to 100 km. Additionally, a benchmark of a linear feed-forward equalizer (FFE) in the optical domain is evaluated. The nonlinear reservoir outperforms the benchmark and reduces the errors into a third on average.

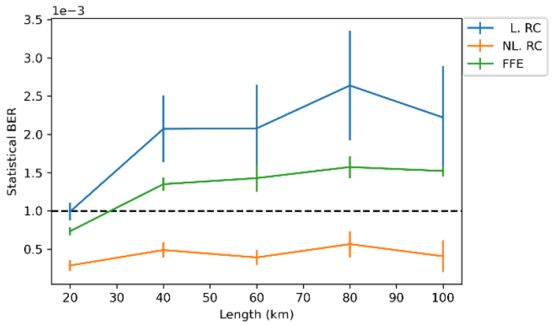

Figure 3: Testing BER vs link length for Linear Reservoir (blue) where no external nonlinearity is present, Nonlinear Reservoir (orange) where the KK receiver is leveraged as a nonlinear block, and an optical Feed Forward Equalizer (green) for benchmarking [53].

ESR12 is working on a photonic implementation of RC based on frequency multiplexing whose schematic is shown on Figure 4, where different neurons are encoded in the complex amplitudes of the lines of a frequency comb. One of the benchmark task on which the network has been successfully tested, both experimentally and in simulation [54], is the nonlinear channel equalization problem based on the model proposed in [31]. Although these first results are positive, they are based on a simplified model of a nonlinearly channel. As next step, the system performances will be evaluated on real world data.

ESR14 has been working on the characterization of the nonlinearities in a SMF with the objective of signal recovery after nonlinear distortion with a reservoir computing device. It is the continuation of the work in [47] where they plan to have the optical reservoir directly performing the data recovery task at the receiver without converting to electric domain. The work was assisted by ESR13 when he was on his secondment.

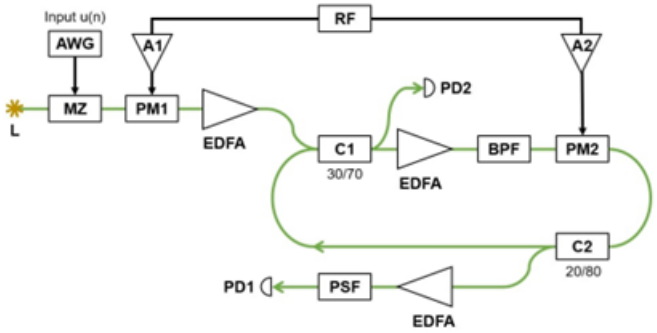

Figure 4: Photonic RC based on frequency multiplexing [54].
Black lines: electrical connections. Green lines: polarization maintaining optical fiber. L: laser. AWG: Arbitrary Waveform Generator. MZ: Mach Zehnder modulator. PM1 and PM2: Phase Modulators. EDFA: Erbium Doped Fiber Amplifier. A1 and A2: RF Amplifiers. C1 and C2: Couplers. BPF: Band Pass Filter. PSF: Programmable Spectral Filter. PD1 and PD2: Photodiodes.

A 50km telecommunication channel has been mounted in the nonlinear photonic lab at IFISC. A 1550nm semiconductor laser was used to generate a continuous-wave signal and sent into a 50km SMF. A 92GSa/s arbitrary waveform generator AWG was used to generate the electric signal for modulation of the continuous wave through a MZM. In order to fit the requirement of the MZM in terms of electrical power, a 20GHz RF amplifier was employed. Also, an erbium-doped fiber amplifier (EDFA) was used at the fiber input to amplify the optical signal to maintain enough power in such a long fiber. For detection at the channel end, a power detector was employed coupled with an optical attenuator to stay below the burning threshold of the detector. The detected electric signal was then sent to a 40GHz oscilloscope to analyze and collect data.

The modulation scheme is chosen with either two or four levels of pulse amplitude modulation (PAM and PAM4). The modulation scheme signal is uploaded into the AWG. It is then applied to the optical signal generated from a high-power laser via the intensity modulator. The EDFA amplifies the modulated signal; a photodetector then detects the filtered output signal before being recorded by the oscilloscope. We aim to reproduce conditions where the optical power is sufficiently high enough to trigger enough non-linearities along the fiber. These high launch power conditions can be interesting in applications such as intra-datacenter transmission to avoid amplification at the receiver and keep only passive components.

To characterize the amount of distortion inside the fiber, a straightforward way is to compute the correlation of the time series. We expect only linear distortion at low launched power, e.g., chromatic dispersion. By increasing the launched power, non-linear distortion occurs; it is interesting to measure the correlation between time series that suffered only from dispersion and transmission that suffered from dispersion and non-linearity. An other way to characterize the non-linearity was a straightforward comparison of the timeseries. It is expected that the peaks of the signal will be reduced and the power . The ultimate test, has been to use the data obtained for a signal recovery task, comparing two approaches. A non-linear approach consisting of using a simulated time-delay reservoir computing, and a linear using only the reservoir computer's output stage, i.e., linear regression. We can compare these two approaches for high power transmission e.g., nonlinearly distorted signal and low power transmission e.g., for linear distortion, in the expectation that the in the first case the non-linear approach should give a better result than the linear one, and in the latter case it should give similar results.

Many parameters have been tuned to compare the different metrics described previously, such as the symbol rate, the launched power, the amplifier gain, the bias current of the laser, the bias voltage of the MZM and the filter of the oscilloscope. After comparison of the metrics described previously, by tuning the different parameters, two key parameters have been shown to be needed for triggering non-linearity in the fiber; modulation speed has to be high enough typically 28 GBaud, as well as the launched power in the fiber typically above 11 dBm. For these typical parameters a significant decrease in the correlation between the low launched power and the high launched power. Furthermore, the bit recovery task for PAM4 modulation, showed a reduction in the BER from of 3 orders of magnitude between the nonlinear recovery ($10^{-}5$) and the linear recovery ($10^{-}3$) after optimization of the MZM bias voltage.

References

[1] Danijela Marković, Alice Mizrahi, Damien Querlioz, and Julie Grollier. Physics for neuromorphic computing. *Nature Reviews Physics*, 2(9):499–510, 2020.

[2] Bhavin J Shastri, Alexander N Tait, T Ferreira de Lima, Wolfram HP Pernice, Harish Bhaskaran, C David Wright, and Paul R Prucnal. Photonics for artificial intelligence and neuromorphic computing. *Nature Photonics*, 15(2):102–114, 2021.

[3] Bhavin J Shastri, Alexander N Tait, Thomas Ferreira de Lima, Mitchell A Nahmias, Hsuan-Tung Peng, and Paul R Prucnal. Principles of neuromorphic photonics. *arXiv preprint arXiv:1801.00016*, 2017.

[4] Alberto Prieto, Beatriz Prieto, Eva Martinez Ortigosa, Eduardo Ros, Francisco Pelayo, Julio Ortega, and Ignacio Rojas. Neural networks: An overview of early research, current frameworks and new challenges. *Neurocomputing*, 214:242–268, 2016.

[5] Qiming Zhang, Haoyi Yu, Martina Barbiero, Baokai Wang, and Min Gu. Artificial neural networks enabled by nanophotonics. *Light: Science & Applications*, 8(1):1–14, 2019.

[6] Thomas Ferreira De Lima, Hsuan-Tung Peng, Alexander N Tait, Mitchell A Nahmias, Heidi B Miller, Bhavin J Shastri, and Paul R Prucnal. Machine learning with neuromorphic photonics. *Journal of Lightwave Technology*, 37(5):1515–1534, 2019.

[7] Nadezhda Semenova, Xavier Porte, Louis Andreoli, Maxime Jacquot, Laurent Larger, and Daniel Brunner. Fundamental aspects of noise in analog-hardware neural networks. *Chaos: An Interdisciplinary Journal of Nonlinear Science*, 29(10):103128, 2019.

[8] Guy Van der Sande, Daniel Brunner, and Miguel C Soriano. Advances in photonic reservoir computing. *Nanophotonics*, 6(3):561–576, 2017.

[9] Gouhei Tanaka, Toshiyuki Yamane, Jean Benoit Héroux, Ryosho Nakane, Naoki Kanazawa, Seiji Takeda, Hidetoshi Numata, Daiju Nakano, and Akira Hirose. Recent advances in physical reservoir computing: A review. *Neural Networks*, 115:100–123, 2019.

[10] Govind P Agrawal. *Fiber-Optic Communication Systems*. Wiley, 5th edition, 2021.

[11] Yuji Kodama. Optical solitons in a monomode fiber. *Journal of Statistical Physics*, 39(5):597–614, 1985.

[12] Alessio Ferrari, Antonio Napoli, Johannes K Fischer, Nelson Costa, Andrea D'Amico, João Pedro, Wladek Forysiak, Erwan Pincemin, Andrew Lord, Alexandros Stavdas, et al. Assessment on the achievable throughput of multi-band itu-t g. 652. d fiber transmission systems. *Journal of Lightwave Technology*, 38(16):4279–4291, 2020.

[13] Claude Elwood Shannon. A mathematical theory of communication. *The Bell system technical journal*, 27(3):379–423, 1948.

[14] René-Jean Essiambre, Gerhard Kramer, Peter J Winzer, Gerard J Foschini, and Bernhard Goebel. Capacity limits of optical fiber networks. *Journal of Lightwave Technology*, 28(4):662–701, 2010.

[15] John C. Cartledge, Fernando P. Guiomar, Frank R. Kschischang, Gabriele Liga, and Metodi P. Yankov. Digital signal processing for fiber nonlinearities [Invited]. *Optics Express*, 25(3):1916–1936, Feb 2017.

[16] Oleg V Sinkin, Ronald Holzlöhner, John Zweck, and Curtis R Menyuk. Optimization of the split-step fourier method in modeling optical-fiber communications systems. *Journal of lightwave technology*, 21(1):61, 2003.

[17] David S Millar, Sergejs Makovejs, Carsten Behrens, Stephan Hellerbrand, Robert I Killey, Polina Bayvel, and Seb J Savory. Mitigation of fiber nonlinearity using a digital coherent receiver. *IEEE Journal of Selected Topics in Quantum Electronics*, 16(5):1217–1226, 2010.

[18] Oscar E Agazzi and Venugopal Gopinathan. The impact of nonlinearity on electronic dispersion compensation of optical channels. In *Optical Fiber Communication Conference*, page TuG6. Optica Publishing Group, 2004.

[19] SJ Savory, Y Benlachtar, RI Killey, P Bayvel, G Bosco, P Poggiolini, J Prat, and M Omella. Imdd transmission over 1,040 km of standard single-mode fiber at 10gbit/s using a one-sample-per-bit reduced-complexity mlse receiver. In *OFC/NFOEC 2007-2007 Conference on Optical Fiber Communication and the National Fiber Optic Engineers Conference*, pages 1–3. IEEE, 2007.

[20] Theodor Kupfer, Claus Dorschky, Mihai Ene, and Stefan Langenbach. Measurement of the performance of 16-states mlse digital equalizer with different optical modulation formats. In *Optical Fiber Communication Conference*, page PDP13. Optica Publishing Group, 2008.

[21] Sergio Benedetto, Ezio Biglieri, and Riccardo Daffara. Modeling and performance evaluation of nonlinear satellite links-a volterra series approach. *IEEE Transactions on Aerospace and Electronic Systems*, (4):494–507, 1979.

[22] Fernando P Guiomar, Jacklyn D Reis, António L Teixeira, and Armando N Pinto. Mitigation of intra-channel nonlinearities using a frequency-domain volterra series equalizer. *Optics express*, 20(2):1360–1369, 2012.

[23] Junho Cho and Son Thai Le. Volterra equalization to compensate for transceiver nonlinearity: Performance and pitfalls. In *2022 Optical Fiber Communications Conference and Exhibition (OFC)*, pages 1–3. IEEE, 2022.

[24] Ezra Ip and Joseph M Kahn. Compensation of dispersion and nonlinear impairments using digital backpropagation. *Journal of Lightwave Technology*, 26(20):3416–3425, 2008.

[25] Antonio Napoli et al. Reduced complexity digital back-propagation methods for optical communication systems. *Journal of lightwave technology*, 32(7):1351–1362, 2014.

[26] Likai Zhu and Guifang Li. Nonlinearity compensation using dispersion-folded digital backward propagation. *Optics express*, 20(13):14362–14370, 2012.

[27] Danish Rafique, Marco Mussolin, Marco Forzati, Jonas Mårtensson, Mohsan N Chugtai, and Andrew D Ellis. Compensation of intra-channel nonlinear fibre impairments using simplified digital back-propagation algorithm. *Optics express*, 19(10):9453–9460, 2011.

[28] Pedro J. Freire, Vladislav Neskornuik, Antonio Napoli, Bernhard Spinnler, Nelson Costa, Ginni Khanna, Emilio Riccardi, Jaroslaw E. Prilepsky, and Sergei K. Turitsyn. Complex-valued neural network design for mitigation of signal distortions in optical links. *Journal of Lightwave Technology*, 39(6):1696–1705, 2021.

[29] Herbert Jaeger. The “echo state” approach to analysing and training recurrent neural networks-with an erratum note. *Bonn, Germany: German National Research Center for Information Technology GMD Technical Report*, 148(34):13, 2001.

[30] Wolfgang Maass, Thomas Natschläger, and Henry Markram. Real-time computing without stable states: A new framework for neural computation based on perturbations. *Neural computation*, 14(11):2531–2560, 2002.

[31] Herbert Jaeger and Harald Haas. Harnessing nonlinearity: Predicting chaotic systems and saving energy in wireless communication. *science*, 304(5667):78–80, 2004.

[32] Mantas Lukoševičius, Herbert Jaeger, and Benjamin Schrauwen. Reservoir computing trends. *KI-Künstliche Intelligenz*, 26(4):365–371, 2012.

[33] Kristof Vandoorne, Wouter Dierckx, Benjamin Schrauwen, David Verstraeten, Roel Baets, Peter Bienstman, and Jan Van Campenhout. Toward optical signal processing using photonic reservoir computing. *Optics express*, 16(15):11182–11192, 2008.

[34] Kristof Vandoorne, Martin Fiers, Thomas Van Vaerenbergh, David Verstraeten, Benjamin Schrauwen, Joni Dambre, and Peter Bienstman. Advances in photonic reservoir computing on an integrated platform. In *2011 13th International Conference on Transparent Optical Networks*, pages 1–4. IEEE, 2011.

[35] Kristof Vandoorne, Joni Dambre, David Verstraeten, Benjamin Schrauwen, and Peter Bienstman. Parallel reservoir computing using optical amplifiers. *IEEE transactions on neural networks*, 22(9):1469–1481, 2011.

[36] Kristof Vandoorne, Pauline Mechet, Thomas Van Vaerenbergh, Martin Fiers, Geert Morthier, David Verstraeten, Benjamin Schrauwen, Joni Dambre, and Peter Bienstman. Experimental demonstration of reservoir computing on a silicon photonics chip. *Nature communications*, 5(1):1–6, 2014.

[37] Ali Rodan and Peter Tino. Minimum complexity echo state network. *IEEE transactions on neural networks*, 22(1):131–144, 2010.

[38] Lennert Appeltant, Miguel Cornelles Soriano, Guy Van der Sande, Jan Danckaert, Serge Massar, Joni Dambre, Benjamin Schrauwen, Claudio R Mirasso, and Ingo Fischer. Information processing using a single dynamical node as complex system. *Nature communications*, 2(1):1–6, 2011.

[39] Yvan Paquot, Francois Duport, Antoneo Smerieri, Joni Dambre, Benjamin Schrauwen, Marc Haelterman, and Serge Massar. Optoelectronic reservoir computing. *Scientific reports*, 2(1):1–6, 2012.

[40] Laurent Larger, Miguel C Soriano, Daniel Brunner, Lennert Appeltant, Jose M Gutiérrez, Luis Pesquera, Claudio R Mirasso, and Ingo Fischer. Photonic information processing beyond turing: an optoelectronic implementation of reservoir computing. *Optics express*, 20(3):3241–3249, 2012.

[41] Piotr Antonik, François Duport, Michiel Hermans, Anteo Smerieri, Marc Haelterman, and Serge Massar. Online training of an opto-electronic reservoir computer applied to real-time channel equalization. *IEEE Transactions on Neural Networks and Learning Systems*, 28(11):2686–2698, 2016.

[42] François Duport, Bendix Schneider, Anteo Smerieri, Marc Haelterman, and Serge Massar. All-optical reservoir computing. *Optics express*, 20(20):22783–22795, 2012.

[43] Daniel Brunner, Miguel C Soriano, Claudio R Mirasso, and Ingo Fischer. Parallel photonic information processing at gigabyte per second data rates using transient states. *Nature communications*, 4(1):1–7, 2013.

[44] Mariia Sorokina, Sergey Sergeyev, and Sergei Turitsyn. Fiber echo state network analogue for high-bandwidth dual-quadrature signal processing. *Optics express*, 27(3):2387–2395, 2019.

[45] Mariia Sorokina. Dispersion-managed fiber echo state network analogue with high (including thz) bandwidth. *Journal of Lightwave Technology*, 38(12):3209–3213, 2020.

[46] François Duport, Anteo Smerieri, Akram Akrout, Marc Haelterman, and Serge Massar. Fully analogue photonic reservoir computer. *Scientific reports*, 6(1):1–12, 2016.

[47] Apostolos Argyris, Julián Bueno, and Ingo Fischer. Photonic machine learning implementation for signal recovery in optical communications. *Scientific reports*, 8(1):1–13, 2018.

[48] Apostolos Argyris, Javier Cantero, M Galletero, Ernesto Pereda, Claudio R Mirasso, Ingo Fischer, and Miguel C Soriano. Comparison of photonic reservoir computing systems for fiber transmission equalization. *IEEE Journal of Selected Topics in Quantum Electronics*, 26(1):1–9, 2019.

[49] Apostolos Argyris, Julian Bueno, and Ingo Fischer. Pam-4 transmission at 1550 nm using photonic reservoir computing post-processing. *IEEE Access*, 7:37017–37025, 2019.

[50] Irene Estébanez, Janek Schwind, Ingo Fischer, and Apostolos Argyris. Accelerating photonic computing by bandwidth enhancement of a time-delay reservoir. *Nanophotonics*, 9(13):4163–4171, 2020.

[51] Mariia Sorokina. Multi-channel optical neuromorphic processor for frequency-multiplexed signals. *Journal of Physics: Photonics*, 3(1):014002, 2020.

[52] Stijn Sackesyn, Chonghuai Ma, Joni Dambre, and Peter Bienstman. Experimental realization of integrated photonic reservoir computing for nonlinear fiber distortion compensation. *Optics Express*, 29(20):30991–30997, 2021.

[53] Sarah Masaad, Emmanuel Gooskens, Stijn Sackesyn, Joni Dambre, and Peter Bienstman. Photonic reservoir computing for nonlinear equalization of 64-qam signals with a kramers–kronig receiver. *Nanophotonics*, 2022.

[54] Lorenz Butschek, Akram Akrout, Evangelia Dimitriadou, Alessandro Lupo, Marc Haelterman, and Serge Massar. Photonic reservoir computer based on frequency multiplexing. *Optics Letters*, 47(4):782–785, 2022.

